Experimental study of optical second-harmonic scattering from spherical nanoparticles

J. Shan,[1] J. I. Dadap,[2] I. Stiopkin,[2] G. A. Reider,[3] and T. F. Heinz[2]
[1]*Department of Physics, Case Western Reserve University, Cleveland, Ohio 44106, USA*
[2]*Departments of Physics and Electrical Engineering, Columbia University, New York, New York 10027, USA*
[3]*Technical University of Vienna, Gusshausstrasse 27, A-1040 Wien, Austria*
(Received 17 May 2005; published 23 February 2006)

Optical second-harmonic (SH) generation from the surface of spherical particles of radii much smaller than the optical wavelength has been investigated experimentally. Angle- and polarization-resolved measurements from dye-coated polystyrene spheres have been obtained for radii of 55 and 85 nm. The SH signals obey general axial- and polarization-selection rules. The polarization-resolved angular patterns agree with the electromagnetic theory of SH Rayleigh scattering that describes the process in terms of locally excited quadrupolar and nonlocally excited dipolar emission. The experimental results differ significantly from those predicted for a local dipole-allowed SH scattering process.

DOI: 10.1103/PhysRevA.73.023819 PACS number(s): 42.65.Ky, 78.67.−n, 78.68.+m

I. INTRODUCTION

The second-order nonlinear optical processes of second-harmonic generation (SHG) and sum-frequency generation (SFG) are well-established probes of surfaces and interfaces [1]. Their inherent interface sensitivity for centrosymmetric media has lead to their use in a wide range of applications. Most of these studies have involved investigations of planar interfaces, for which the nonlinear optics problem of excitation and radiation has been solved and thoroughly tested. Recently, however, SHG and SFG have also been found to be very useful probes of the surfaces of small particles [2–11]. Corresponding theoretical analyses of the nonlinear response of spherical particles [5,10–16], as well as for dilute and concentrated suspensions of spherical particles [17], have been developed. In the important Rayleigh limit of particle radii small compared to the wavelength of light, a simple analytic solution to the general problem has been derived [13–15]. This solution makes specific predictions about polarization selection rules and angular scattering patterns, as well as scaling laws with respect to frequency and particle size. The features of this process, which reflect the strong cancellation effects present in a centrosymmetric object, require consideration of propagation effects even in the Rayleigh limit. The resulting SH emission includes a dipole contribution, but, unlike the linear optical response, with a nonlocal excitation mechanism yielding a dipole moment lying in the axial direction. In addition, theory predicts the presence of a quadrupole radiation term, which, in contrast to the linear case, is of the same order as the dipole term.

Here we present an experimental study of SH radiation for a model system of spherical particles of radii as small as 55 nm. These investigations are directed to verification of the intriguing characteristics predicted by the explicit analytic theory available for SH scattering in the Rayleigh limit. The work is motivated by the growing body of experimental work in which SHG and SFG have been applied to examine the surfaces and interfaces of particles. These investigations range from probing molecular adsorption and transport [2–7] to studies of surface charging effects [8,9] and of the interfaces of nanoscale inclusions in solid matrices [11]. The nonlinear response of nanoscale objects is also critical for approaches to near-field optical microscopy and spectroscopy that have been developed using SHG [18]. The present experiment complements studies of the characteristics of SHG by nanoparticles, including the size [19,20] and spectral dependence [21], the effect of sample and field inhomogeneities [11], and radiation patterns of nonspherical particles [22]. It also extends studies of angular dependence of nonlinear scattering from micron-sized particles [4,5,8] to the nanometer length scale. Our experimental investigations demonstrate distinctive polarization and angular selection rules for the SH Rayleigh scattering (SHRS). These selection rules are completely at variance with those obeyed by linear Rayleigh scattering (LRS), but emerge naturally from the electromagnetic theory of SHRS [13–15]. Detailed angular dependences of the SH scattering are also reported. These data are found to be compatible with the predictions of the SHRS theory and, with a modest finite-size correction, excellent quantitative agreement is obtained. The results show that the fluctuation-induced process of hyper-Rayleigh scattering (HRS), omitted from the continuum analysis, does not make a significant contribution to the measured response from particles of radii as small as 55 nm. These investigations constitute a careful test of the analytic electromagnetic theory of SHRS and highlight the marked qualitative differences with respect to the familiar linear optical analog.

II. EXPERIMENT

To investigate the SHRS process experimentally, we made use of monodispersed ($<10\%$ spread) polystyrene spheres of 55 and 85 nm radii suspended in water (Polysciences, Inc.). The concentration (10^{16}–10^{17} m^{-3}) was sufficiently low to ensure that the radiation from the ensemble was simply the incoherent sum of the single-particle response and that multiple-scattering effects could be neglected. To enhance the surface nonlinear response, malachite green (MG) dye was introduced to form an adsorbed monolayer on the surface of the spheres. Care was taken to prevent aggregation of the particles and dimerization of the dye molecules by choos-

TABLE I. Maximal measured SHRS signal strengths for the indicated polarization configurations and for the axial geometry for 55-nm-radius particles. H and V denote, respectively, horizontally and vertically polarized radiation with respect to the scattering plane. The values are normalized to the $V \rightarrow H$ signal. The predicted selection rules for both SHRS and LRS are shown for comparison.

Experimental configuration	SHRS		LRS
	Experimental	Theory	
$V \rightarrow H$	1.0	Allowed	Forbidden
$H \rightarrow H$	0.9	Allowed	Allowed
$H \rightarrow V$	<0.10	Forbidden	Forbidden
$V \rightarrow V$	<0.10	Forbidden	Allowed
$\theta=0°$, 180°	<0.02	Forbidden	Allowed

ing appropriate MG concentration ($\sim \mu M$) and solution pH (~ 5).

The laser source for the measurements was a mode-locked Ti:sapphire oscillator, which provided 60-fs pulses at a wavelength of 820 nm and an average power of 300 mW. The detection system consisted of gated photon counting in combination with appropriate narrowband interference filters. We recorded the dependence of SH signal on the scattering angle θ from the direction $\hat{\mathbf{k}}$ of the incoming radiation by rotating the detector about the spherical sample cell. Better than 5° angular resolution was achieved. Measurements were made for the five polarization configurations of $H \rightarrow V$, $V \rightarrow V$, $H \rightarrow H$, $V \rightarrow H$, and $C \rightarrow T$. Here H denotes a direction in the scattering plane, V the direction perpendicular to it, T the total signal (without polarization analysis), and C corresponds to circular polarization.

The SH emission from nanoparticles in MG solution arose predominantly from their dye-coated surfaces. The particles themselves, without the MG adlayer, gave rise to negligible SH response. The MG molecules in the solution without the spheres did produce weak SH radiation through the hyper-Rayleigh scattering process. This contribution is incoherent with respect to the desired SHRS signal; it was measured separately and has been subtracted off in the data presented below. To eliminate any angular nonuniformity in the detection sensitivity, we normalized the SHRS by the isotropic $V \rightarrow V$ two-photon fluorescence from the MG molecules in solution that could be measured at a redshifted wavelength compared to the SH signal.

III. RESULTS AND ANALYSIS

Before we report the full SH angular and polarization data, we present results for the principal polarization configurations. Table I summarizes the maximum values for each of the configurations. We find that the polarization combinations of $V \rightarrow H$ and $H \rightarrow H$ produce substantial and roughly comparable SH emission, while the $H \rightarrow V$ and $V \rightarrow V$ configurations yield no SH signal within experimental accuracy ($<10\%$ of the peak signal). Further, no SH radiation is emitted, to experimental accuracy ($<5\%$ of the peak signal), for all polarization combinations in either the forward ($\theta=0°$) or backward ($\theta=180°$, by extrapolating the data) axial direction.

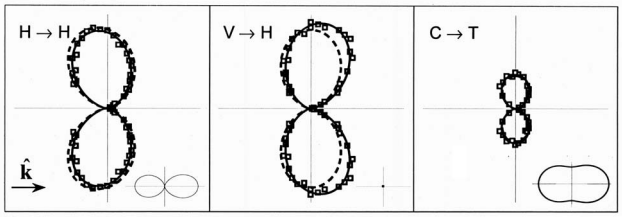

FIG. 1. Polar plot of the dependence of SH radiation on the scattering angle θ for a suspension of dye-coated spheres of 55-nm radius. The experimental data (symbols) were collected for θ in the range of [0, 180°], but are also shown for the equivalent range of [180°, 360°] for clarity. The forward scattering direction is designated by the unit wave vector $\hat{\mathbf{k}}$ of the incident radiation. Results are indicated in the three panels for the $H \rightarrow H$, $V \rightarrow H$, and $C \rightarrow T$ polarization configurations. The scales reflect the detected SH signal. The dotted lines are generated by the SHRS model of Eq. (1) using a single set of parameters χ_1 and χ_2; the solid lines include a finite-size correction. The theory is adjusted for the measured ratio of the SH detection sensitivity for V- and H-polarized radiation. For comparison, the corresponding linear optical scattering patterns are shown as insets.

It is instructive to compare the nonlinear SHRS process to conventional LRS. For SHRS, the $H \rightarrow V$ and $V \rightarrow V$ configurations are forbidden. For LRS, no radiation is observed in cases where the output and input beam polarizations are orthogonal, i.e., $H \rightarrow V$ and $V \rightarrow H$. Thus, the absence of $H \rightarrow V$ scattering is common to both processes. On the other hand, $V \rightarrow V$ scattering is prohibited for SHRS, but corresponds to strong scattering for LRS. Conversely, while $V \rightarrow H$ scattering is forbidden for LRS, this configuration yields strong SH scattering. In addition, in terms of the dependence on the scattering angle, the LRS signal is maximal along the forward and backward axial directions, where the SHRS is found to vanish. These differences can be understood qualitatively by recognizing that for LRS, a dipole moment is induced parallel to the exciting electric field; for the SHRS process, however, phase shifts are needed to make the process symmetry allowed. This causes the SHRS process to produce dipole emission from a moment parallel, rather than perpendicular to the direction of propagation of the pump beam.

The polarization and axial selection rules found experimentally, and summarized in Table I, follow from the explicit theoretical results obtained for SHRS [13–15]. The polarization selection rules are a direct consequence of *mirror symmetry in the scattering plane* for an object producing a second-order nonlinear response. Similarly, the absence of SH radiation in the axial directions follows directly from the *π-rotation symmetry* of the object about $\hat{\mathbf{k}}$. These selection rules, therefore, are restricted neither to the Rayleigh limit nor to scattering from spheres, but require only the presence of the relevant symmetry of the SH scatterer.

Figures 1 and 2 display the measured SH radiation patterns as a function of the scattering angle θ for spheres of

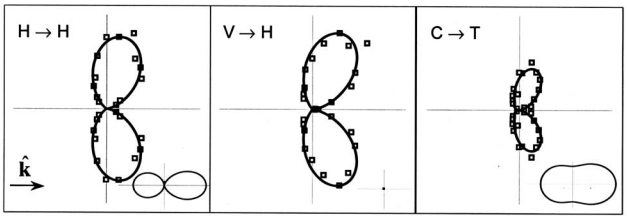

FIG. 2. As in Fig. 1, but for particles of 85-nm radius.

55 nm and 85 nm radii. The panels in each figure correspond, respectively, to the symmetry-allowed $H \rightarrow H$, $V \rightarrow H$, and $C \rightarrow T$ polarization configurations. The $C \rightarrow T$ configuration is included because of its simple interpretation in terms of the SH sources, as we discuss below. The insets indicate the corresponding radiation patterns for LRS (including a leading-order finite-size correction). The SHRS and LRS patterns are qualitatively different. In addition to the distinct polarization selection rules just described, LRS is peaked in the axial directions, while radiation lobes for the SHRS are directed near the $\theta=90°$ direction. Although the angular patterns vary somewhat with particle size (compare Figs. 1 and 2), the most striking effect is the relative magnitude of the signals in the two cases. We find that the SH signal is ~11 times greater for scattering from an 85-nm sphere than for scattering from a 55-nm sphere.

We now compare the experimental results to theory. The model we employ is that of a spherical object of isotropic, centrosymmetric material with a nonlinear response described by a surface nonlinear susceptibility tensor $\vec{\vec{\chi}}_s^{(2)}$. This formulation is analogous to the well-established model for the planar geometry. Within the Rayleigh limit, the scattered electric field at the SH frequency (2ω) measured at a distance r from the sphere of radius a is given by [13,14]

$$\mathbf{E}^{(2\omega)}(\mathbf{r}) = \frac{8\pi i K^2 a^3 E_0^2}{15}\frac{\exp(iK_1 r)}{r}[k_1\chi_1(\hat{\boldsymbol{\varepsilon}}_0\cdot\hat{\boldsymbol{\varepsilon}}_0)(\hat{\mathbf{K}}\times\hat{\mathbf{k}})\times\hat{\mathbf{K}} - K_1\chi_2(\hat{\mathbf{K}}\cdot\hat{\boldsymbol{\varepsilon}}_0)(\hat{\mathbf{K}}\times\hat{\boldsymbol{\varepsilon}}_0)\times\hat{\mathbf{K}}]. \quad (1)$$

Here E_0, $\hat{\mathbf{k}}$, and $\hat{\boldsymbol{\varepsilon}}_0$ are the amplitude, unit wave vector, and polarization of the exciting electric field, respectively; $\hat{\mathbf{K}}$ is the direction of observation for the scattered SH radiation; $k_1=k\varepsilon^{1/2}$ and $K_1=K\varepsilon^{1/2}(2\omega)$ denote the amplitude of the wave vector of the fundamental and SH radiation in the surrounding medium of dielectric constant ε. The complex coefficients χ_1 and χ_2 are linear combinations of the tensor elements of the surface nonlinear susceptibility $\vec{\vec{\chi}}_s^{(2)}$ weighted by appropriate local-field factors [13,14]. As we see from Eq. (1), the SH radiation has both electric-dipole and electric-quadrupole emission terms. The strengths of these two terms, and consequently all angular and polarization dependences of the SH radiation, are determined by the two coefficients χ_1 and χ_2. Since we are generally not concerned with the absolute phase of the SH emission, the radiation is actually defined by just three real parameters: the magnitudes $|\chi_1|$, $|\chi_2|$, and the relative phase $\arg(\chi_2/\chi_1)$. The specific predictions of Eq. (1) for the angular dependence of the SH power per unit solid angle $d\mathcal{P}_{2\omega}/d\Omega$ are indicated in Table II for the symmetry-allowed polarization combinations. Note that the electric-dipole and electric-quadrupole radiation modes are isolated, respectively, for the $V \rightarrow H$ and $C \rightarrow T$ configurations.

TABLE II. Dependence of the predicted SHRS as a function of scattering angle θ for selected symmetry-allowed polarization configurations. H, V, C, and T denote, respectively, horizontally, vertically, circularly polarized radiation, and the total radiation.

Polarization configuration	Predicted angular dependence of SH power: $d\mathcal{P}_{2\omega}/d\Omega \propto \lvert\mathbf{E}^{(2\omega)}(\mathbf{r})\rvert^2$
$H \rightarrow H$	$\lvert 2k_1\chi_1 \sin\theta + K_1\chi_2 \sin 2\theta\rvert^2$
$V \rightarrow H$	$\lvert 2k_1\chi_1 \sin\theta\rvert^2$
$C \rightarrow T$	$\lvert K_1\chi_2\rvert^2(1-\cos^4\theta)$

We have employed Eq. (1) to fit the three measured radiation patterns for the 55-nm-radius particle in Fig. 1 (symbols) simultaneously. With just one overall strength parameter and the complex ratio χ_2/χ_1 of the two susceptibilities, the SHRS theory (dotted lines) is seen to reproduce the features of the radiation patterns. Inspection reveals a small departure of the experiment from theory. For example, the SHRS theory predicts purely electric-dipole radiation ($V \rightarrow H$ configuration) to peak at $\theta=90°$. Experimentally the radiation lobe is directed slightly in the forward direction at $\theta \approx 80°$. This departure reflects the finite size of the spheres and the need to treat propagation effects more accurately; it can be accounted for analytically by higher-order expansions in (Ka), as described in Appendix A of [14]. Including the next nonvanishing $[(Ka)^5]$ correction terms in the SH field, as shown by the solid lines in Fig. 1, we obtain excellent agreement with experiment. The correction introduces all three independent tensor elements of $\vec{\vec{\chi}}_s^{(2)}$, with two complex parameters determining the angular dependence of SH scattering. The correction to the SH field, estimated at $\theta=90°$ for the $V \rightarrow H$ polarization configuration, is ~12%. From the fitting procedure, we obtain ratios of $|\chi_2/\chi_1|=0.26$ and 0.22 for the SHRS and the modified theory, respectively.

The SH radiation patterns for the 85-nm-radius spheres (Fig. 2, symbols) maintain the same characteristic features as for the smaller spheres, but show a more pronounced tendency towards forward scattering, as is also evident for the $C \rightarrow T$ data. This behavior is an indication of a more significant finite-size effect. Including a modest leading-order $(Ka)^5$ correction, however, still produces good agreement with experiment (Fig. 2, solid lines). The dominant role of the simple SHRS scattering process is evident in a comparison of the SH response for the 55 nm and 85 nm spheres. From Eq. (1), we expect the SH intensity to scale as a^6 with particle radius. Experimentally, we find the ratio of the peak signals for the 85-nm-radius and 55-nm-radius particles to be ~11. This would imply a ratio of the radii of the particles in SHRS theory of $11^{1/6} \cong 1.49$, in close accord with the experimental ratio of the two radii of $(85/55) \cong 1.55$.

IV. DISCUSSION

The SHRS analysis considered above does not allow for any local electric-dipole nonlinear response of the particles.

This is rigorously valid for a fully centrosymmetric object, such as the ideal homogeneous spherical particles assumed in the model. Inversion symmetry is obviously broken when the particles are made of a noncentrosymmetric material, and strong SH scattering has been observed from nanoparticles of noncentrosymmetric materials such as CdSe and CdS [20]. Even for nominally centrosymmetric systems like ours, weaker symmetry breaking from distortions in the shape of the nanoparticles or surface inhomogeneity from the random disposition of the adsorbed molecules is present to some degree and will allow local-dipole SH emission [22]. Our experimental data for 55-nm-radius particles are, however, incompatible with a local dipole contribution. A contribution of this type would yield nonzero response for the $V \rightarrow V$ configuration and an isotropic response in the scattering plane for the $V \rightarrow H$ configuration [23], in contradiction with experiment. The crossover from the observed regime of SHRS described by the continuum response to the regime of hyper-Rayleigh scattering from fluctuations in the molecular adlayer can be estimated to occur for particles of radius $\sim(d/k_1)^{1/2}$, where d is the mean separation between the molecules. For $d=1$ nm, the fluctuation-induced response is expected to dominate for particles of radius <10 nm, defining the regime where a continuum description of the nonlinear response ceases to be appropriate.

ACKNOWLEDGMENTS

This work was sponsored at Columbia University by MRSEC Program of the NSF under Grant No. DMR-0213574 and by the U.S. DOE, Office of Basic Energy Sciences, through the Catalysis Science Grant No. DE-FG03-03ER15463, and at Case Western Reserve University by the NSF under Grant No. DMR-0349201.

[1] See, for example, G. A. Reider and T. F. Heinz, in *Photonic Probes of Surfaces*, edited by P. Halevi (Elsevier, Amsterdam, 1995), pp. 413–478; P. F. Brevet, *Surface Second Harmonic Generation* (Presses Polytechniques et Universitaires Romandes, Lausanne, 1997).
[2] H. Wang *et al.*, Chem. Phys. Lett. **259**, 15 (1996).
[3] A. Srivastava and K. B. Eisenthal, Chem. Phys. Lett. **292**, 345 (1998).
[4] N. Yang, W. E. Angerer, and A. G. Yodh, Phys. Rev. Lett. **87**, 103902 (2001).
[5] S. Roke, W. G. Roeterdink, J. E. G. J. Wijnhoven, A. V. Petukhov, A. W. Kleyn, and M. Bonn, Phys. Rev. Lett. **91**, 258302 (2003).
[6] J. M. Hartings *et al.*, Chem. Phys. Lett. **281**, 389 (1997).
[7] H. F. Wang *et al.*, Langmuir **16**, 2475 (2000).
[8] V. Boutou *et al.*, Opt. Lett. **30**, 759 (2005).
[9] E. C. Y. Yan, Y. Liu, and K. B. Eisenthal, J. Phys. Chem. B **102**, 6331 (1998).
[10] J. Martorell, R. Vilaseca, and R. Corbalán, Phys. Rev. A **55**, 4520 (1997).
[11] Y. Jiang *et al.*, Appl. Phys. Lett. **78**, 766 (2001); Y. Jiang, L. Sun, and M. C. Downer, *ibid.* **81**, 3034 (2002); P. Figliozzi, L. Sun, Y. Jiang, N. Matlis, B. Mattern, M. C. Downer, S. P. Withrow, C. W. White, W. L. Mochan, and B. S. Mendoza, Phys. Rev. Lett. **94**, 047401 (2005).
[12] G. S. Agarwal and S. S. Jha, Solid State Commun. **41**, 499 (1982).
[13] J. I. Dadap, J. Shan, K. B. Eisenthal, and T. F. Heinz, Phys. Rev. Lett. **83**, 4045 (1999).
[14] J. I. Dadap, J. Shan, and T. F. Heinz, J. Opt. Soc. Am. B **21**, 1328 (2004).
[15] V. L. Brudny, B. S. Mendoza, and W. L. Mochán, Phys. Rev. B **62**, 11152 (2000); W. L. Mochán, J. A. Maytorena, B. S. Mendoza, and V. L. Brundy, *ibid.* **68**, 085318 (2003).
[16] D. Östling, P. Stampfli, and K. H. Bennemann, Z. Phys. D: At., Mol. Clusters **28**, 169 (1993); J. P. Dewitz, W. Hübner, and K. H. Bennemann, *ibid.* **37**, 75 (1996); Y. Pavlyukh and W. Hübner, Phys. Rev. B **70**, 245434 (2004).
[17] E. V. Makeev and S. E. Skipetrov, Opt. Commun. **224**, 139 (2003).
[18] A. Bouhelier, M. Beversluis, A. Hartschuh, and L. Novotny, Phys. Rev. Lett. **90**, 013903 (2003); C. C. Neacsu, G. A. Reider, and M. B. Raschke, Phys. Rev. B **71**, 201402(R) (2005).
[19] O. A. Aktsipetrov, P. V. Elyutin, A. A. Nikulin, and E. A. Ostrovskaya, Phys. Rev. B **51**, 17591 (1995).
[20] See for example, M. Jacobsohn and U. Banin, J. Phys. Chem. B **104**, 1 (2000); Y. Zhang *et al.*, J. Phys. Chem. Solids **64**, 927 (2003).
[21] E. C. Hao *et al.*, J. Chem. Phys. **117**, 5963 (2002); R. C. Johnson *et al.*, Chem. Phys. Lett. **356**, 534 (2002).
[22] J. Nappa, G. Revillod, I. Russier-Antoine, E. Benichou, C. Jonin, and P. F. Brevet, Phys. Rev. B **71**, 165407 (2005).
[23] R. Bersohn, Y. H. Pao, and H. L. Frisch, J. Chem. Phys. **45**, 3184 (1966).